Clays and Clay Minerals, Vol. 54, No. 6, 653–666, 2006.

A NEW Ni-RICH STEVENSITE FROM THE OPHIOLITE COMPLEX OF OTHRYS, CENTRAL GREECE

GEORGE E. CHRISTIDIS[1,*] AND IOANNIS MITSIS[2]

[1] Technical University of Crete, Department of Mineral Resources Engineering, 73100, Chania, Greece
[2] Section of Geochemistry and Economic Geology, Department of Geology, University of Athens, Panepistimioupolis, Ano Ilisia 15784, Greece

Abstract—The first occurrence of Ni-rich stevensite found in the ophiolite complex of Othrys, Central Greece is described. The stevensite, which develops in cracks in a host serpentinite, formed at the expense of serpentine. Two varieties of stevensite have been described: a Mg-rich, Ni-poorer variety with 0.4−1.2 octahedral Ni atoms per half formula unit (p.h.f.u.) and a Ni-rich variety with >2 Ni atoms p.h.f.u. The layer charge in both varieties is −0.24 p.h.f.u.. Stevensite layers are completely separated when dispersed in dilute polyvinylpyrrolidone (PVP) solutions and begin to convert to talc after heating at 250ºC for 90 min. Total conversion to talc is observed at 550ºC. Formation of Ni-rich stevensite took place at ambient temperature during supergene processes. The scarcity of Ni-rich stevensite occurrences in nature is attributed to the metastability of smectite and to the analytical procedures used in previous studies. Stevensite is considered a phase containing domains with variable numbers of octahedral vacancies. A new experimental protocol is proposed for the determination of Ni-rich stevensite, based on a combination of XRD after solvation with various organic liquids and subsequent heating at 750ºC.

Key Words—Greece, Metastability, Ni-rich Stevensite, Octahedral Vacancy, Othrys Ophiolite Complex, PVP, Serpentine, Supergene Alteration, Talc, XRD.

INTRODUCTION

Smectites form in a wide variety of geological environments including hydrothermal alteration, diagenesis and supergene processes such as weathering and low-temperature water-rock interaction (Grim and Güven, 1978; Golightly, 1981; Decarreau *et al.*, 1987; Chamley, 1989; Christidis, 2001, among many others). In these environments smectite is usually an alteration product of a precursor phase, either a mineral (*e.g.* feldspar, pyroxene, olivine) or an X-ray amorphous phase (volcanic glass), usually *via* an intermediate gel-like precursor. It may form either as a pure phase constituting the main mineral of clayey rocks known as bentonites (Grim and Güven, 1978) or as a mixed-layer phase with other phyllosilicate components such as illite, kaolinite, chlorite, talc and serpentine (Eberl *et al.*, 1982; Środoń and Eberl, 1984; Herbillon *et al.*, 1981; Beaufort and Meunier, 1994; Inoue *et al.*, 2004; Sakharov *et al.*, 2004, among many others). In these environments the smectite chemistry usually displays considerable variation due to significant variations in the micro-environmental conditions (Christidis and Dunham, 1993, 1997), although there are exceptions to this trend (Christidis, 2001).

The crystal chemical characteristics of smectites are dictated by the nature of the precursor phase, the composition of the fluid phase and the nature of the geological processes in which they form. Thus, Mg-rich smectites like saponite and stevensite usually form from alteration of basic-ultrabasic rocks or in saline lake deposits often associated with evaporites (Eberl *et al.*, 1982; Jones and Weir, 1983; Bodine and Madsen, 1987). Fe-rich montmorillonites beidellites and nontronites form *via* palagonitization (Zhou and Fyfe, 1989), during hydrothermal processes both on the sea floor (Alt, 1999) and in subaerial environments (Brigatti, 1983) and during weathering processes such as lateritization of basic-ultrabasic rocks (Bosio *et al.*, 1975; Paquet *et al.*, 1982; Dubinska, 1986; Wilson, 1987; Decarreau *et al.*, 1987). In nickeliferous laterites, nontronite and Fe-rich montmorillonite are usually concentrated within and above the saprolite zone (Golightly, 1981) and are often nickeliferous (Bosio *et al.*, 1975; Nahon *et al.*, 1982; Dubinska, 1986; Gaudin *et al.*, 2004a).

The main trioctahedral Ni-bearing phyllosilicate formed in weathering profiles of ultrabasic rocks is disordered Ni-rich talc (pimelite according to Brindley and Maksimovic, 1974), which forms intimate mixtures with Ni-rich serpentine known as garnierites (Brindley and Hang, 1973; Brindley *et al.*, 1979; Paquet *et al.*, 1982; Gerard and Herbillon, 1983). Pimelite-like layers in nickeliferous laterites have been reported to coexist with Ni-free nontronite (*e.g.* Decarreau *et al.*, 1987). Nontronite and pimelite-like layers have been found to form mixed trioctahedral and dioctahedral domains, whereby Ni is hosted in the trioctahedral component (Decarreau *et al.*, 1987). According to Manceau *et al.* (1985) the crystal field stabilization energy (CFSE) of Ni

* E-mail address of corresponding author:
christid@mred.tuc.gr
DOI: 10.1346/CCMN.2006.0540601

in stevensite is ~1 kcal/mole less than the pimelite, but according to Güven (1988) this may not be sufficient to explain the formation of pimelite instead of Ni-rich stevensite.

Trioctahedral smectites with either tetrahedral or octahedral charge (Ni-rich saponite and Ni-rich stevensite, respectively) and variable Mg/Ni ratios have been synthesized at low temperatures in the laboratory (Decarreau, 1985). Although the partition coefficient for Ni (D_{Ni-Mg}) between the octahedral sheet of smectite and water is 1000 (Decarreau, 1985), smectite with Ni as the predominant octahedral cation (*i.e.* trioctahedral smectite) has not been observed in nature (*e.g.* Güven, 1988). In general, Ni in natural Ni-rich smectites occupies a limited number of octahedral sites, which does not exceed 0.40 atoms p.h.f.u. (Brindley and Souza, 1975; Bosio *et al.*, 1975; Dubinska, 1986; Gaudin *et al.*, 2004a) and in most cases the Ni occupancy does not exceed 0.2 atoms p.h.f.u. (see Dubinska, 1986, and Gaudin *et al.*, 2004a, for reviews). This has been attributed to the dioctahedral nature of these smectites (nontronites-Fe-montmorillonites) which precludes the segregation of Ni atoms in dioctahedral domains (Gaudin *et al.*, 2004b). It is interesting that Ni-rich smectites in lateritic profiles are dioctahedral (Ni-bearing nontronites or Fe-Ni montmorillonites).

In this work we describe the first occurrence of a stevensite with Ni as the predominant octahedral cation, formed during supergene alteration at low temperature, and discovered in the ophiolite complex of Othrys, in central Greece. It is the purpose of this contribution to present the mechanism of formation of this Ni-rich smectite and discuss the possible reasons for the general absence of trioctahedral Ni-rich smectites during supergene alteration of ultrabasic rocks. We also propose an alternative analytical protocol for verification of Ni-rich stevensite found in such geological environments.

GEOLOGICAL FRAMEWORK-SAMPLING SITE

The Mesozoic Othrys ophiolite complex, central Greece (Figure 1) consists mainly of lherzolites, hartzburgites, gabbros, mafic dikes and pillow lavas (Hynes, 1972; Menzies, 1974; Nisbet, 1974; Konstantopoulou and Rasios, 1993; Dijkstra *et al.*, 2001). The study area is located in the area of Ano Agoriani, in the western sector of Othrys Mountain and is dominated by serpentinized plagioclase-lherzolite (Menzies, 1973; Courtin, 1979; Dijkstra *et al.*, 2001) (Figure 1). The geological framework of the study area is given by Mitsis and Economou-Eliopoulos (2001). Minor Ni mineralization associated with hydrothermal alteration characterized by heazlewoodite and pentlandite as well as supergene Ni mineralization characterized by reevesite, Ni-rich chlorite, Ni-rich serpentine, Ni-rich talc and associated magnetite and apatite occurs in the tectonic

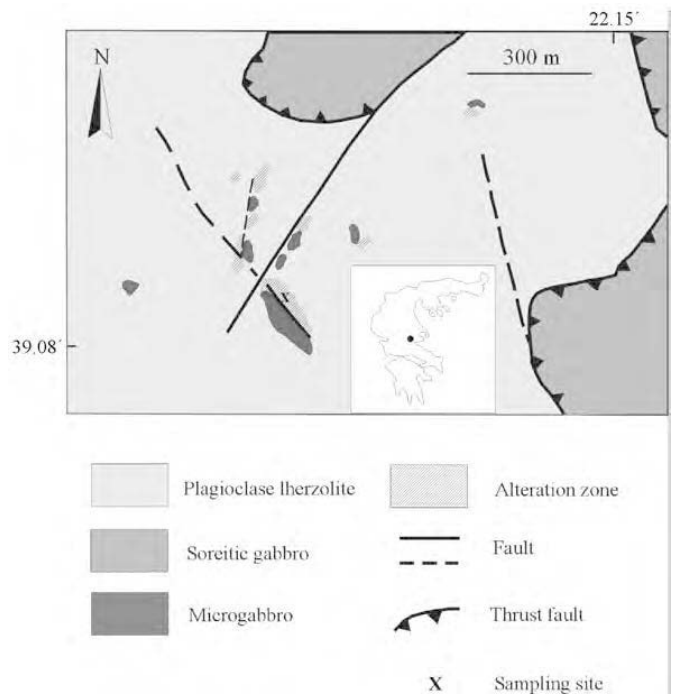

Figure 1. Geological map of the study area.

https://doi.org/10.1346/CCMN.2006.0540601 Published online by Cambridge University Press

contact between overlying serpentinized plagioclase-lherzolite and underlying microgabbros (Mitsis, 2001) (Figure 2). In these supergene zones, veinlets 1–30 mm wide occur, especially along the tectonic contact, in areas where the serpentinized lherzolite is extensively altered and friable. These veinlets, which are filled with secondary sheet silicates, form in stockwork textures within serpentinite and in larger veins at greater depths within serpentinite.

MATERIALS AND METHODS

The Ni-bearing samples were collected from thin veinlets which crosscut serpentinites. The samples display a range of green colors from bright green to dark green-blue depending on their Ni content. Previous work has shown that bright green samples are softer and have a significantly greater Ni content than the dark green ones (Mitsis, 2001). Bulk mineralogy was determined by powder X-ray diffraction (XRD) (Siemens D8000, CuKα radiation, graphite monochromator, 35 kV and 35 mA, using a 0.02º step size and 1 s per step counting time), on randomly oriented samples initially crushed with a hammer and subsequently ground with pestle and mortar. The clay mineralogy was determined in materials dispersed in distilled water using an ultrasonic probe (20 s). The <2 μm fractions were separated by settling, dried on Si wafers at room temperature and then were solvated with ethylene glycol vapor at 60ºC overnight to ensure maximum saturation. The XRD traces of the clay fractions were obtained both from the air-dried and the ethylene glycol-solvated clay fractions using a 0.02º step size and 4 s per step counting time.

Selected samples were heated at 250, 550, 750 and 1000ºC and examined by XRD in order to determine the thermal transformations of the phyllosilicates. In addition, the clay fractions of the samples heated at 250, 550 and 750ºC were separated, spread on Si wafers, saturated with ethylene glycol and examined by XRD. Selected clay fractions were dispersed in aqueous solutions which contained polyvinylpyrrolidone (molecular weight 55,000, referred to as PVP-55K). At low smectite-solution ratios, PVP molecules can separate 10 Å smectite particles so that interparticle diffraction is eliminated and only the structure factor is visible (Eberl *et al.*, 1998; Blum and Eberl, 2004). Total separation can occur also if some isolated layers of a phase, which cannot intercalate PVP, such as illite, talc or kerolite, are mixed with smectite layers (Eberl *et al.*, 1998). The use of PVP-55K would assist in distinguishing pure smectite from any possible mixed-layer phase with random interlayering that may be present, which would contain smectite as a major component and stacks of layers of a phase which does not intercalate PVP such as illite and talc. The clay:PVP ratio used was 2 mg clay/mL. Such a ratio is sufficiently low to allow excess PVP molecules to separate smectite particles if present (Blum and Eberl, 2004).

Gold-coated broken surfaces of representative samples were examined with a JEOL JSM-5400 SEM, equipped with an Oxford Link energy dispersive spectrometer (EDS) for qualitative analyses, in order to determine the textural relationships between the various minerals present in the samples. Back-scattered electron (BSE) images were used to study the morphological differences between the Ni-rich and the Mg-rich phases before and after heating. Three representative samples with variable green color and thus different Ni contents were saturated with 1 M $CaCl_2$. Ca was selected as an index cation because the samples are Ca free. Subsequently, the samples were centrifuged and the supernatant solution was analyzed for Mg, Ni and Co.

The clay fractions of selected samples in the air-dried state and after heating at 750ºC were examined with infrared (IR) spectroscopy using a Perkin Elmer 1000 Fourier transform infrared (FTIR) spectrometer in the range 400–4000 cm^{-1}. Each spectrum was the average of 50 scans collected at 4 cm^{-1} resolution. 1.5 mg of the clay fractions was diluted in 200 mg of KBr and pressed

Figure 2. Development of the shear zone (Sz) at the contact between the serpentinized plagioclase lherzolite (Ser) and microgabbro (Mgb). The exact location of the veinlets with smectite is indicated by the arrow. The vertical scale bar in the central bottom part is 1 m long.

https://doi.org/10.1346/CCMN.2006.0540601 Published online by Cambridge University Press

in 13 mm KBr disks, which were subsequently dried at 150ºC for 15 h (Russell, 1987). Differential thermal and thermogravimetric analyses (DTA-TG) were carried out on clay fractions in order to determine the dehydration behavior of clay minerals during heating, using a Setaram DTA-TG analyzer. The samples were heated in Pt crucibles in the range 20−1000ºC with a heating rate of 10ºC/min in a He atmosphere.

Smectite chemistry was determined by electron microprobe analysis (EMPA) of carbon-coated epoxy-impregnated polished blocks, using a JEOL JSM-5600 scanning electron microscope (SEM) equipped with an Oxford Link energy dispersive spectrometer (EDS). Analyses were carried out using 60 s livetime, 20 kV acceleration current potential, and 2 nA sample current. The accuracy, precision and detection limits of the method used were examined by Dunham and Wilkinson (1978). The absolute error for 68% of analyses is ±0.32% for all oxides whereas the relative error for 68% of analyses is ±2.3% for oxide concentrations >1% and ±1.9% for oxide concentrations >5%. In general, the accuracy and precision is comparable to the wavelength dispersive spectrometers but the detection limits are greater. All selected points were analyzed for Si, Ti, Al, Fe, Ni, Co, Mn, Mg, Ca, Na and K. Measured concentrations were automatically corrected for atomic number, absorption in the sample fluorescence, and dead time (the ZAF correction), using the ISIS 300 software of Link. The concentrations of Ti, Al, Fe, Mn, Ca, Na and K were always below the detection limit of the instrument. Therefore the system studied is essentially free of Al and Fe and can be described geochemically by the relative abundances of Si, Mg and Ni. The structural formulae of the smectites were obtained using 11 oxygen atoms (half formula unit) with the following assignments: Si was assigned to tetrahedral sites and Mg, Ni and Co were assigned to octahedral sites. From each analysis, an amount of MgO equal to that displaced by $CaCl_2$ was considered as exchangeable Mg, and subsequently was subtracted from the total Mg and assigned to interlayer sites. This is considered an optimum approximation because it is not possible to differentiate between octahedral and exchangeable Mg solely from EMPA analysis (*e.g.* Christidis and Dunham, 1993, 1997). As smectite is not characterized by heterovalent substitutions in either the tetrahedral or the octahedral sheet, the layer charge stems from vacancies, mainly in the octahedral sheet.

Chemical analyses of representative bulk samples were carried out by digestion of 1000 mg of finely powdered sample in a high-pressure TFM Teflon vessel using an ETHOS 1600 MILESTONE microwave system. Only light-green colored samples (light-green color is indicative of the presence of Ni) were selected. The samples were digested with a mixture of 3 mL of HCl (37%), 2 mL of HNO_3 (65%), 1.5 mL of HF (40%) and 5 mL of H_3BO_3 (5%). After digestion the solution was diluted to proper volume with distilled water. Si, Mg, Ni, Co, Al, Fe, Ca, Fe, Cr and Cu concentrations were determined using a Perkin Elmer 1100b atomic absorption spectrophotometer. Loss on ignition (LOI) was determined after heating at 1000ºC without any pre-treatment, *i.e.* without pre-drying at 105ºC.

RESULTS

Mineralogy and mineral textures

Powder XRD results show that the samples consist of an 11−12 Å phyllosilicate phase and minor serpentine (trace 1 in Figure 3). The 060 reflections of the 11−12 Å phase and serpentine (1.525 Å) are practically inseparable suggesting that both phases are trioctahedral, without dioctahedral components. Moreover the existence of the 020 band is indicative of turbostratic structure, typical of smectites (Figure 3). The oriented clay fractions also display the 11−12 Å phase and a 7 Å phase, identified as serpentine (Figure 4a). Inasmuch as smectite with exchangeable Mg is expected to yield a 001 diffraction maximum at 14−15 Å, it follows that a mixed-layer phase containing a smectitic and a non-

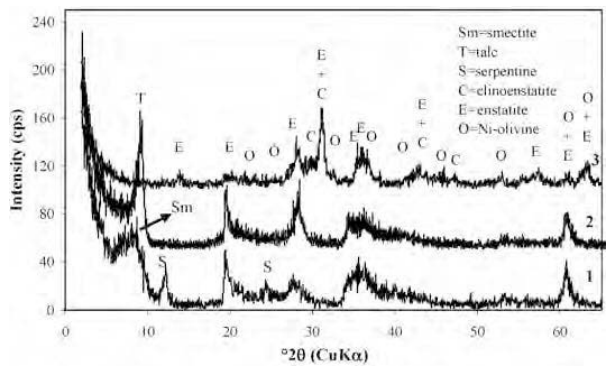

Figure 3. Random XRD traces of the original smectitic clay (1) and its equivalent heated at 750ºC (2) and 1000ºC for 90 min (3).

https://doi.org/10.1346/CCMN.2006.0540601 Published online by Cambridge University Press

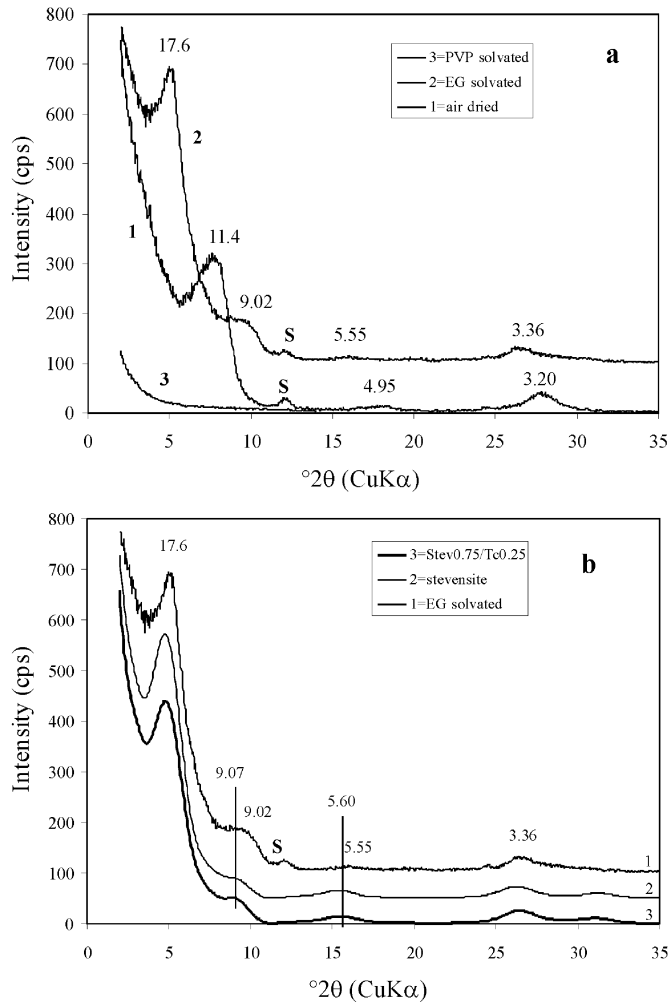

Figure 4. (a) XRD traces of the clay fraction of the smectite-rich clay. S = serpentine. (b) Experimental and simulated XRD traces of ethylene glycol-solvated clay fractions using NEWMOD©. 1 = experimental trace, 2 = simulated XRD trace of stevensite with one layer mean defect-free distance and CSD consisting of 1–5 layers. Bold line = simulated XRD trace of mixed-layer stevensite-talc (0.75/0.25). *d* spacings are in Å.

swelling component may be present. After saturation with ethylene glycol, the reflection at 11–12 Å migrated to 17.6 Å suggesting that the phase contains an expandable component corresponding to smectite. In the ethylene glycol-solvated samples, the lack of 9.6 Å phase indicates the lack of discrete talc or its poorly crystallized equivalent kerolite. Prolonged ultrasonic treatment for 1 min may enhance the swelling behavior of talc-like phases, although the swelling of talc-like minerals differs from that of smectites (Wiewióra *et al.*, 1982). In the present study, ultrasonic treatment was limited to 20 s. Moreover, the XRD characteristics of the studied samples strongly suggest that the predominant phase is smectite (Figure 4) in contrast to Wiewióra *et al.* (1982).

The 001 diffraction maximum of the ethylene glycol-solvated samples at ~17.6 Å is characterized by considerable peak broadening, a high saddle at the low-angle side and irrational higher-order basal spacings (Figure 4a). Such XRD characteristics, which have been reported by Brindley *et al.* (1977) for stevensite layers, may also indicate the presence of random interstratification between smectite and another 2:1 phyllosilicate, probably talc, because the possibility of a mica component is ruled out by the chemical composition of the mineral (see below). Randomly interstratified kerolite-

https://doi.org/10.1346/CCMN.2006.0540601 Published online by Cambridge University Press

stevensite is a rather common phase (Eberl *et al.*, 1982) and in fact stevensite has been visualized as a mixture of domains of smectite with octahedral vacancies and kerolite without octahedral vacancies (Shimoda, 1971; see also Güven, 1988, for a review). X-ray diffraction trace modeling with NEWMOD (Reynolds and Reynolds, 1996), using pure trioctahedral smectite layers with coherent scattering domains (CSD) consisting of 1−5 layers and one layer mean defect-free distance, reproduced the experimental traces (line 2 in Figure 4b). However, modeling with NEWMOD using an R0 mixed-layer trioctahedral smectite-kerolite with 75% smectite layers yielded similar results (bold line in Figure 4b). Therefore, although the difference between pure smectite and kerolite is the existence or lack of swelling after ethylene glycol solvation (Brindley *et al.*, 1977), such a treatment cannot allow unequivocal distinction between smectite and R0 mixed-layer smectite-talc with a high proportion of smectite.

In order to resolve this ambiguity, we treated smectite with PVP-55K having a 2 mg of clay/1 mL of solution concentration. If pure smectite is present in the samples, then interparticle diffraction will be eliminated and only the structure factor will appear in the XRD traces (Blum and Eberl, 2004). If R0 mixed-layer smectite-talc is present, talc particles will be visible due to complete separation of the smectite layers after PVP treatment, unless single talc or kerolite layers are isolated within smectite layers (Eberl *et al.*, 1998). Intercalation with PVP-55K showed that in most samples, talc or kerolite particles containing several stacked layers are not present (Figure 4a). Therefore the observed peak broadening, the high saddle/background ratio of the 001 diffraction maximum and the irrational higher-order basal reflections observed after ethylene glycol solvation are attributed to the minute smectite crystallite size, the small number of smectite layers per CSD and/or the presence of isolated talc layers within the smectite layers.

Under the SEM, smectite forms elongated, flattened, wavy flakes, which in places form honeycomb structures (Figure 5a,b). Qualitative EDS analyses showed that smectite consists only of Si, Mg and Ni, with Mg and Ni being present at variable proportions, with Mg dominat-

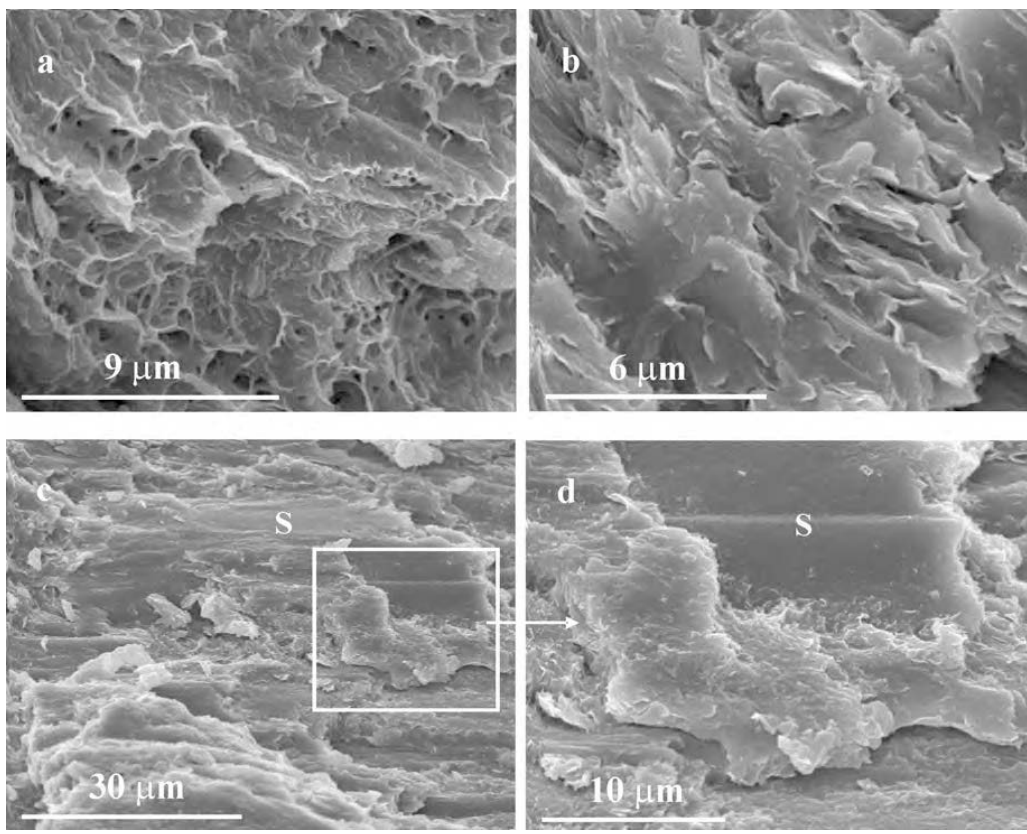

Figure 5. SEM images of the smectitic clays. S = serpentine. See text for discussion.

https://doi.org/10.1346/CCMN.2006.0540601 Published online by Cambridge University Press

ing over Ni. Most importantly, the smectites are devoid of Al and Fe. This indicates that neither saponite nor griffithite is present. Therefore, this is an additional indication for the presence of stevensite. Smectite has formed at the expense of another Mg phyllosilicate leading to pseudomorphic replacement (Figure 5c,d). Although stevensite can be formed at the expense of olivine by experimental weathering (Manceau *et al.*, 1985), the mineralogical composition of the samples and the surrounding rocks, which are olivine-free, indicate that in this study, trioctahedral smectite formed at the expense of serpentine.

Back scattered electron (BSE) images show that the Ni-rich phases form small bright lath-like domains, embedded in a Ni-bearing, Mg-rich matrix, which consists of thin, continuous, sub-parallel laths, separated into brighter and darker domains (Figure 6a,b). The brighter domains are richer in Ni. Locally, small cracks, attributed to desiccation of the materials under high vacuum, are present (Figure 6b). The boundaries between the Ni-rich laths and the Ni-poorer matrix are sharp and so are the boundaries between the Ni-poor and the Ni-rich domains of the matrix. These textures remain essentially unchanged after heating at 750ºC (Figure 7).

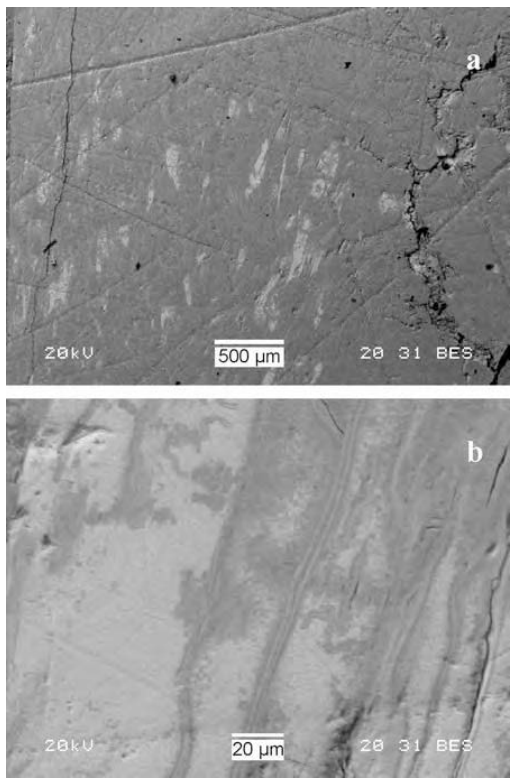

Figure 6. BSE images of the original smectitic clays.

In parts of the Mg-richer matrix of the heated samples, small domains develop, ~10 µm in diameter, with abundant shrinkage cracks. These domains, which resemble the macroscopic 'pop corn' shrinkage textures often observed after wetting and drying of smectites in the field, are richer in Ni than the surrounding matrix, but poorer in Ni than the bright Ni-rich laths.

Thermal treatment and IR results

Progressive heating of smectite in the temperature range 250–1000ºC for 90 min leads to gradual decrease of the swelling layers and formation of non-swelling talc layers (Figure 8). At 250ºC a fraction of expandable (*i.e.* smectite) layers still exists, but at 550ºC, smectite layers are absent (Figure 8). With increasing temperature, the diffraction maxima of talc become narrower and sharper and their intensity increases suggesting increasing crystal order (Figures 3, 8). Above 800ºC, enstatite forms, and at 1000ºC an olivine-like phase is also present (trace 3 in Figure 3). Manceau *et al.* (1985) described the conversion of synthetic Ni-bearing smectites to Ni-bearing pimelite after heating at 165ºC. Also, Brindley *et al.* (1977) found that air-dried oriented stevensite collapsed to 9.4 Å after heating at 350ºC. However, the duration of the heating in those studies was not mentioned. The DTA-TG analysis showed a substantial weight loss between 50 and 200ºC, attributed to loss of interlayer and adsorbed water, a first endothermic event at ~600ºC and a second main endothermic event at 800ºC followed by an exothermic one, attributed to the dehydroxylation of talc and the formation of enstatite, respectively. The endothermic event at 600ºC is attributed to the dehydroxylation of serpentine and the smectite (Shimoda, 1971).

The FTIR spectra of the original clay fractions and their equivalents after heating at 750ºC, corresponding to sample 3 in Table 2 (see below) are shown in Figure 9. The spectra have noticeable differences both in the OH-stretching region and in the region of lattice vibrations, strongly suggesting that they consist of different phases. In the OH-stretching region the heated samples contain four bands typical of nickeliferous talc, namely 3678, 3662, 3646 and 3626 cm^{-1}, which are assigned to $Mg_3(OH)$, $Mg_2Ni(OH)$, $MgNi_2(OH)$ and $Ni_3(OH)$, respectively (Wilkins and Ito, 1967). The original smectite is characterized by four bands at 3678, 3660, 3652 and 3626 cm^{-1} and a small shoulder at 3631 cm^{-1}. The bands at 3678 and 3631 cm^{-1} are comparable with the bands reported by Shimoda (1971) for stevensite (3685 and 3630 cm^{-1}). Thus the main difference in the FTIR spectra of the original and the heated samples is the intense band at 3652 cm^{-1} in the former, which can be attributed to $MgNi_2(OH)$ stretching in stevensite.

In the region of lattice vibrations, the FTIR spectra of the original clay fractions are broader and tend to be non-symmetric, while the bands of the heated samples

https://doi.org/10.1346/CCMN.2006.0540601 Published online by Cambridge University Press

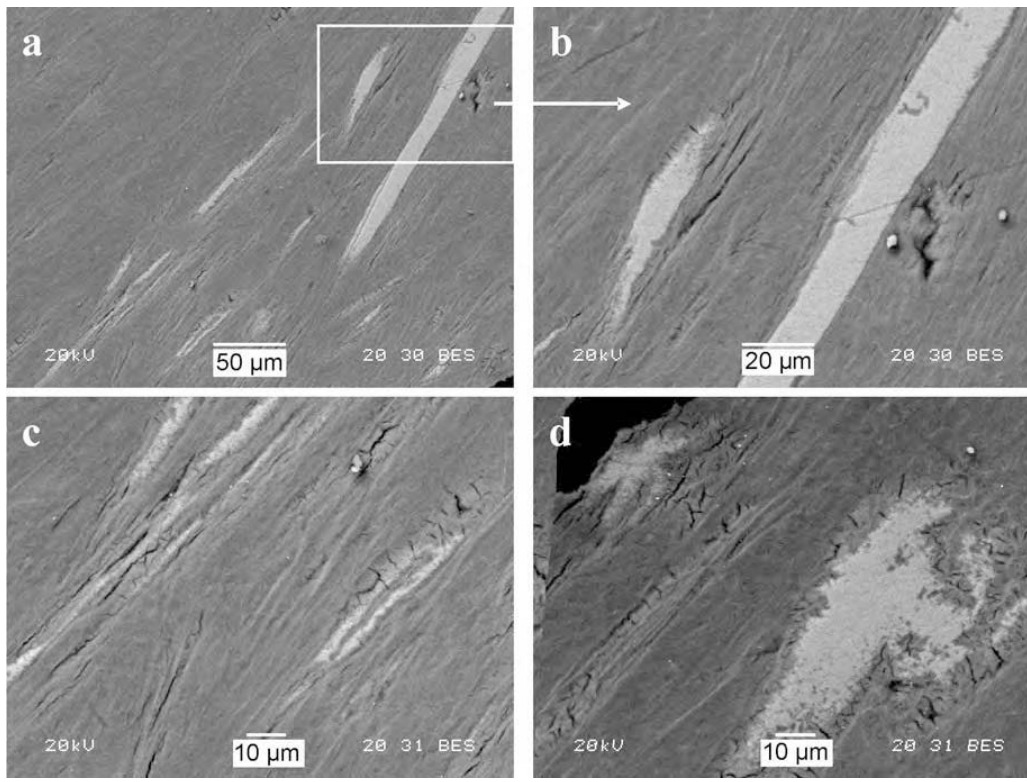

Figure 7. BSE images of the smectitic clays heated at 750ºC for 90 min.

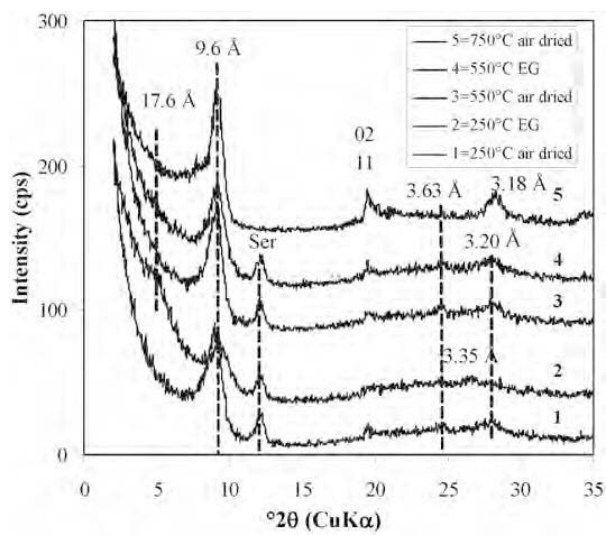

Figure 8. XRD traces of the smectitic clays heated at 250 and 550ºC (oriented samples) and 750ºC (random powders) for 90 min. EG = ethylene glycol solvation. Ser: serpentine.

https://doi.org/10.1346/CCMN.2006.0540601 Published online by Cambridge University Press

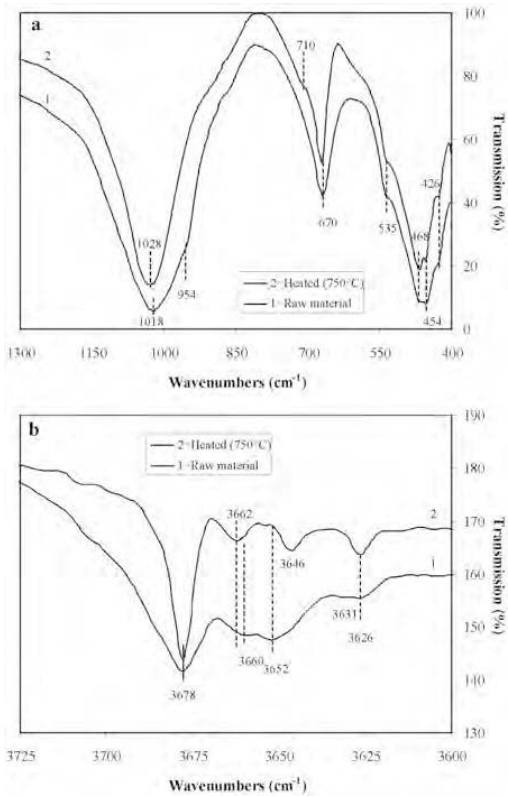

Figure 9. FTIR spectra of the original smectitic clay and the clay heated at 750ºC. (a) OH-stretching region; (b) lattice-vibration region.

are more symmetric, being typical of talc. Hence the bands at 454, 468 and 535 cm^{-1} are attributed to Si–O–R vibration, *R*–O and/or translational OH-vibration and *R*–O vibration respectively, where *R* = Mg and/or Ni and the bands at 426 cm^{-1} to Si–O bending. In the spectrum of the original sample, the relative intensities of the bands at 454 and 468 cm^{-1} are reversed (Figure 9a). Also, next to the librational OH vibration at 670 cm^{-1}, which is present in the original sample, an additional shoulder at 710 cm^{-1} appears in the heated sample. This shoulder is typical of nickeliferous talc and has often been used to quantify the amount of Ni present (Wilkins and Ito, 1967; Gerard and Herbillon, 1983). Finally, in the Si–O stretching region, in the original sample the main band is asymmetric, centered at 1018 cm^{-1} with shoulders at 954, 1063 and 1090 cm^{-1}, whereas in the heated sample, only one band is present, centered at 1028 cm^{-1}. Using the reasoning of Besson *et al.* (1987), we estimated the octahedral Mg and Ni content, assuming a random cation distribution, from the integrated optical densities W_{ijk} of the IR bands at ~3600–3680 cm^{-1} in the heated talc-bearing sample. In this notation *i*, *j* and *k* correspond to the cations which occupy the octahedral sites in the trioctahedral layer. The content of each cation was calculated as the sum of contributions of this cation to the integrated intensities of the bands of those -OH groups, which contain the specific cation in their coordination sphere (Slonimskaya *et al*., 1986). The calculated cation occupancy is 1.75 and 1.25 for Mg and Ni, respectively, corresponding to a Mg:Ni ratio of 0.58:0.42. This ratio is comparable to that calculated from bulk chemical analysis, assuming that it consists of talc instead of stevensite (0.62:0.38). The observed difference is attributed to the fact that the latter refers to the bulk original sample, which consists mainly of stevensite instead of talc and minor serpentine (Figure 3).

Smectite and talc chemistry

Saturation of the original samples with $CaCl_2$ showed that 1.07% of MgO in the Ni-poor samples and 0.95% of MgO in the Ni-rich samples is exchangeable. No exchangeable Ni or Co was detected. These concentrations correspond to 30 meq/100 g and 25.5 meq/100 g on an anhydrous basis, for the Mg-rich and Ni-rich smectites, respectively. This MgO content was subtracted from the total MgO of the Mg-rich and Ni-rich smectites and it was assigned as exchangeable Mg. In contrast, the heated talc-bearing samples do not contain any exchangeable Mg. Average values of the chemical elements and the cation distributions, standard deviations and minimum and maximum values for smectite and talc are listed in Table 1. Smectite is trioctahedral without tetrahedral charge and the layer charge stems from vacancies in the octahedral sheet. This confirms that the smectitic phase is indeed stevensite. There are 0.12 vacant octahedral sites p.h.f.u. on average yielding, a mean layer charge of −0.241. This value is comparable to that observed by Eberl *et al.* (1982) for R0 mixed-layer kerolite-stevensite containing ~80% stevensite and Köster (1982) for a series of stevensites. The endothermic event at 600ºC described before can be tentatively attributed to dehydroxylation of the vacant octahedra.

The octahedral sheet of the stevensite is occupied mainly by Mg and Ni, with small amounts of Co in places. As expected, an almost perfect negative trend holds between Ni and Mg, as Mg is replaced by Ni (Figure 10a). However, the trend is not continuous, rather a gap exists between the Mg-rich and the Ni-rich members. The gap is not attributed to thermodynamic constraints, because experimental work has shown that transition metals including Ni, can replace Mg in octahedral sites of synthetic stevensite without limitations (Decarreau, 1985). Ni-rich stevensite has a greater Co content than its Mg-rich counterparts and stevensite with a smaller Ni content is, in general, Co-free (Figure 10b).

The heated samples contain talc with almost perfect stoichiometry (Table 1). Similar to smectite, Ni replaces Mg yielding a nearly perfect negative trend between the

https://doi.org/10.1346/CCMN.2006.0540601 Published online by Cambridge University Press

Table 1. Average microprobe analyses (wt.%) and structural formulae of the original Ni-rich smectitic clays and their heated counterparts.

	Original material (n = 35)				Heated material (n = 24)			
	Mean	s.d.	max	min	Mean	s.d.	max	min
SiO_2	50.78	3.36	56.69	40.81	57.78	2.98	60.70	50.96
NiO	21.81	11.04	36.33	7.84	17.73	8.66	35.68	8.74
CoO	0.47	0.48	1.32	0.00	0.33	0.39	1.31	0.00
MgO	13.63	7.34	22.64	4.21	19.38	6.32	25.90	5.89
Total	86.69				95.22			
Structural formulae based on 11 O atoms								
Si	3.996	0.005	4.010	3.985	3.998	0.004	4.007	3.993
Ni	1.416	0.767	2.416	0.484	1.015	0.566	2.246	0.463
Co	0.031	0.032	0.088	0.000	0.019	0.024	0.082	0.000
Mg	1.442	0.793	2.400	0.398	1.970	0.586	2.543	0.689
VI cations	2.889	0.010	2.909	2.858	3.004	0.008	3.014	2.985
Mg(exch)*	0.121	0.004	0.131	0.112				
LayCharge	0.241	0.008	0.262	0.225				
IntCharge	0.241	0.008	0.262	0.225				

*Mg(exch) was calculated by subtraction from total MgO based on the CEC of the samples (see text for discussion).
VI cations is sum of octahedral cations
LayCharge = layer charge
IntCharge = interlayer charge

two elements, parallel to that of smectites (Figure 10a). Talc has greater Ni and Mg contents than smectite in the whole range of octahedral compositions, because all Mg was assigned to octahedral sites and no exchangeable Mg was subtracted during calculation of the structural formulae. Again, a gap exists between the Ni-rich and the Mg-rich members of the trend. The Mg-rich members of the trend extend to more Ni-rich compositions compared to stevensite. In contrast, the Ni-rich talc component does not display compositional heterogeneity, but has a virtually constant Ni content. Ni-richer talc has a larger Co content, similar to stevensite.

Bulk chemistry

The results of the chemical analyses are listed in Table 2. The samples are essentially free of Al, Fe, Ca and alkalis and have small Co contents. The Ni and Mg contents of the clay samples vary between broad limits. In contrast, the Si content displays less variability. Also, all samples have high LOI. Although LOI was determined without prior drying, such LOI values are typical of smectite rather than talc. Larger Ni contents are observed in those samples with bright green color, whereas Ni-poor, Mg-rich clays are dark green. The moderately large Ni content is in accordance with the FTIR results and the BSE images (Figure 5, 9), which indicate that the Ni-rich domains are not extensive. Finally, samples richer in Ni have larger Co contents.

DISCUSSION

In this study we presented the first occurrence of Ni-rich stevensite formed at the expense of Ni-rich serpentine via supergene alteration. Two varieties of

Table 2. Bulk chemical compositions (wt.%) of representative Ni-bearing clays with variable Ni content, from Othrys ophiolite complex (Central Greece).

	1	2	3	4	5	6
SiO_2	52.79	52.96	51.90	52.64	54.16	54.12
Al_2O_3	0.08	0.04	0.15	0.15	0.40	0.25
Fe_2O_3	0.03	0.01	0.03	0.04	0.20	0.04
NiO	17.48	16.20	17.22	10.29	8.25	17.01
CoO	0.28	0.28	0.29	0.15	0.13	0.29
CuO	0.01	0.01	0.01	0.01	0.01	0.01
MgO	11.04	13.94	15.72	18.66	19.89	15.74
CaO	0.06	0.06	0.06	0.11	0.11	0.10
LOI	17.36	15.87	14.41	17.46	15.91	11.99
Total	99.12	99.37	99.79	99.51	99.05	99.54

https://doi.org/10.1346/CCMN.2006.0540601 Published online by Cambridge University Press

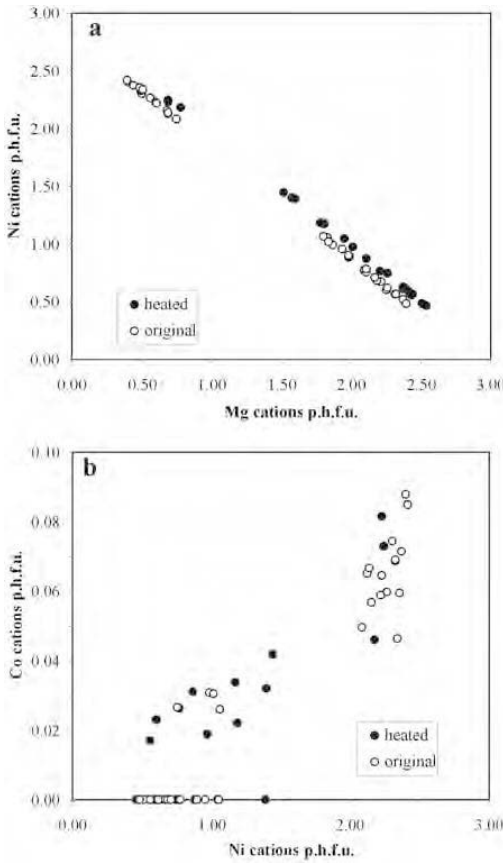

Figure 10. Electron microprobe analyses of the original and heated smectitic clays. (a) octahedral Mg *vs*. octahedral Ni; (b) octahedral Mg *vs*. octahedral Co.

stevensite have been recognized, a Mg-Ni variety with Ni varying between 0.4 and 1 atoms p.h.f.u., and a Ni-ich variety containing >2 Ni atoms p.h.f.u. The Mg-rich, Ni-poor variety dominates. The predominance of Mg-rich stevensite and its heated equivalent talc explains the FTIR spectra which show that ~40% of octahedral sites of the bulk samples are occupied by Ni (Figure 9). The Ni-rich smectite studied was formed in a rather exceptional low-temperature geological environment described essentially by three chemical elements, namely Si, Mg and Ni and the total lack of Fe, Al, Ca and alkalis.

In most samples the swelling trioctahedral layers were completely separated when dispersed in dilute PVP solutions. Based on the reasoning of Blum and Eberl (2004) we considered this behavior as indicative of the existence of pure smectite layers and the lack of talc or kerolite particles several layers thick, because PVP molecules are not expected to separate talc layers in dilute suspensions. However, it is possible that isolated kerolite or its Ni equivalent pimelite layers may be present between Ni-rich stevensite layers. Such layers can also fully expand in dilute PVP solutions. After heating at temperatures as low as 250ºC for 90 min, stevensite layers begin to convert to non-swelling talc-like layers (Figures 3, 8). Although determining the mechanism of this transformation was not the purpose of the present study, the progressive decrease of swelling with increasing heating temperature could well suggest either that the vacant octahedral sites are progressively filled with Mg, or that the vacant octahedral sites are destroyed during heating at 250ºC. In the former alternative, the source of Mg could be invoked in the interlayer sites. Note that the main difference between the talc formed at high temperatures and original stevensite is the greater Mg:Ni ratio in octahedral sites of the latter, although the total MgO content is comparable in the two phases (Table 1). However, an attempt to saturate stevensite with Ca and subsequent heating at 250ºC did not prevent conversion to talc. This indicates that stevensite is not a stable phase and that its conversion to talc does not involve simple migration of exchangeable Mg in vacant octahedral sites, but includes more important structural rearrangements which involve conversion of the turbostratic structure to a more ordered structure. This topic is currently under investigation.

According to CEC measurements and EMPA data, the total net layer charge varies between −0.225 and −0.262 p.h.f.u.. The vast majority of the layer charge is due to octahedral vacancies (Table 1). The smallest total net layer charge is close to the lower charge limit assigned for smectite (−0.20 p.h.f.u.: Bailey, 1980). However, this by no means excludes the possibility that there are layers with smaller or greater layer charges, *i.e.* a smaller or greater number of octahedral vacancies. In fact, the smaller number of octahedral vacancies determined is 0.098 atoms p.h.f.u. yielding an octahedral charge of −0.196 p.h.f.u., although in this particular analysis the total layer charge determined is −0.234 owing to a small tetrahedral vacancy. Such small charge layers are expected to behave more like talc than smectite layers. Hence stevensite may be visualized as a phase with a variable number of octahedral vacancies, which yield smectite-like and talc-like domains. In this sense the mixed-layer stevensite-talc (Eberl *et al.*, 1982) may be alternatively explained as a mixture of smectite-like (stevensite) layers with a variable number of octahedral vacancies and hence variable layer charge. In this case, PVP seems to be more efficient in separating discrete domains of low-charge stevensite layers than other organic molecules such as ethylene glycol.

The IR data may provide information on the distribution of Mg and Ni cations in the octahedral sheet of talc. As noted before, the assumption for random distribution yielded a Mg:Ni ratio of 0.58:0.42 comparable with the chemical analyses of the bulk clay

https://doi.org/10.1346/CCMN.2006.0540601 Published online by Cambridge University Press

fraction. A random cation distribution would yield the relative intensities of the OH-stretching bands listed in Table 3b. However, in Figure 3b the relative intensities of the OH-stretching bands are considerably different. Hence the $Mg_3(OH)$ and $Ni_3(OH)$ bands at 3678 and 3626 cm^{-1}, respectively, are more intense (relative intensities of 0.352 and 0.265, respectively) than the remaining OH-stretching bands and have greater intensities than their counterparts, assuming random distribution (Table 3a). This indicates that the distribution of Mg and Ni atoms is not random, but the cations are clustered in accordance with previous works (Manceau and Calas, 1986; Decarreau *et al.*, 1987). Although in this study there are no data available for cation clustering in stevensite, there is no reason to exclude such a possibility due to the structural similarity of the two phases. This suggests that clustering of Mg and Ni is a characteristic of trioctahedral clay minerals forming during weathering of basic and ultrabasic rocks.

The instability of stevensite layers upon heating indicates that heating at 750ºC, often used to separate pimelite-like layers from serpentine and smectite layers (*e.g*. Gerard and Herbillon, 1983; Decarreau *et al.*, 1987) should be avoided. This is because, although nontronite and serpentine layers will decompose due to dehydroxylation at 500−600ºC, any stevensite layers that may be present will be converted to talc. As an alternative procedure to detect Ni-rich stevensite we suggest the following analytical protocol, which includes: (1) examination by XRD both of randomly oriented powders to determine the di- or trioctahedral nature of the phyllosilicate phases (*i.e*. to distinguish nontronite from stevensite and/or talc); (2) ethylene glycol solvation of oriented clay fractions to distinguish swelling from non-swelling components (*i.e.* smectite from talc and/or serpentine); (3) dispersion in dilute PVP solution (2 mg clay/1 mL of solution) to distinguish pure stevensite from R0 mixed-layer stevensite-kerolite/pimelite and/or discrete kerolite/pimelite stacks; (4) heating at 750ºC to separate pimellite from nontronite if stevensite is absent. If stevensite is still present, heating will simply convert it to talc layers. However, even using this protocol, isolated kerolite and/or pimelite layers within stevensite may not be distinguished from stevensite.

Table 3. Occurrence probabilities of octahedral cations W_{ik} (i,k = Mg and Ni, respectively) in Ni-rich talc formed from heating of Ni-rich stevensite at 750ºC (a) according to the IR data and (b) assuming random distribution of octahedral atoms. The ratio Mg:Ni atoms is 0.58:0.42 corresponding to 1.75 Mg atoms and 1.25 Ni atoms. See text for discussion.

Wavenumber (cm^{-1})	Band assignment	a W_i	b W_i
3678	$Mg_3(OH)$	0.352	0.195
3662	$Mg_2Ni(OH)$	0.155	0.424
3646	$MgNi_2(OH)$	0.228	0.307
3626	$Ni_3(OH)$	0.265	0.074

So far, smectites with Ni as a main octahedral cation have not been observed in nature. Due to the specific geochemical affinity of Ni for mantle-derived rocks, Ni-bearing smectites form as secondary phases during low-temperature processes such as lateritic weathering of ultrabasic rocks (Paquet *et al.*, 1982; Dubinska, 1986; Decarreau *et al.*, 1987). These smectites are nickeliferous nontronites having ferric Fe as the main octahedral cation and a small Ni content, which does not exceed 0.4 atoms p.h.f.u. The nontronites also bind the Al available in the system, while the main trioctahedral phase, which hosts Ni in such environments, is considered to consist of disordered Ni-rich talc-like, *i.e*. pimelite-like layers (Decarreau *et al.*, 1987; see also Güven, 1988, for a review). However, stevensite is a rather common mineral formed in other geological environments such as saline lake deposits often associated with evaporites (Eberl *et al.*, 1982; Jones and Weir, 1983; Bodine and Madsen, 1987). In the present study, disordered talc, either Ni-rich kerolite or pimelite particles have been detected in places in trace amounts only. We attribute the overall scarcity of Ni-rich stevensite to (1) thermodynamic constraints regarding the stability of Ni-rich stevensite and smectite in general; and (2) to the analytical methods used in previous studies.

Previous reports (Lippmann, 1982; May *et al.*, 1986) have considered smectite a metastable phase formed due to kinetic constraints, *i.e*. not due to thermodynamic equilibrium. Thus its formation can be attributed to the Ostwald step rule. The smectite studied is considered a metastable phase because it converts to its stable counterpart, *i.e*. talc, after heating at 250ºC, well below its dehydroxylation temperature (800ºC). Therefore, any stevensite which may form during low-temperature processes (continental saline lakes, supergene processes) will be converted to talc if it is subjected to slightly higher temperatures during diagenesis or to subsequent reheating during a younger magmatic intrusion, probably *via* a mixed-layer stevensite-kerolite phase. Moreover, if abundant Al and Fe are available, then other phases usually found in Ni-rich laterites such as nickeliferous Fe montmorillonite or nontronite, chlorite and saponite will form instead of Ni-rich stevensite. Hence the lack of Al and Fe in the present study prevented the formation of Fe-Al smectites and/or chlorite. The Ni talc-like (pimelite-like) domains described by Decarreau *et al.* (1987) may well correspond to Fe-poor, Ni-rich stevensite, *i.e.* not to talc domains. Note that these authors attributed the swelling of the talc-domains to the small crystallite size (3000 Å or 0.3 μm). However, such a crystallite size is very common for many clay minerals such as illite and kaolinite, which do not swell in ethylene glycol vapor. In

https://doi.org/10.1346/CCMN.2006.0540601 Published online by Cambridge University Press

contrast, Brindley *et al.* (1977) observed that only a small fraction of some kerolites swell after extremely prolonged exposure to ethylene glycol vapor. In this sense, trioctahedral Ni-rich smectites may be more common than previously thought, even in Ni lateritic profiles.

CONCLUSIONS

A new Ni-rich stevensite was discovered in the ophiolitic complex of Othrys, central Greece. The presence of smectite layers, significantly different from talc layers, was verified by a series of independent tests of evidence. These include the existence of cation exchange capacity in the original (smectite) samples, swelling in ethylene glycol vapor, the formation of desiccation cracks in the original sample in high vacuum and dehydration cracks in the samples heated at 750ºC, the small microprobe analysis totals of the original samples, the large LOI values of the original samples, the gradual conversion of smectite to talc after heating at temperatures well below the dehydroxylation temperature, the different FTIR spectra of the original (smectitic) material and heated (talc) material and the complete dispersion of the original samples to dilute PVP solutions. Based on the findings of this work, a new experimental protocol for detecting Ni-rich stevensite is suggested.

ACKNOWLEDGMENTS

The constructive reviews of A. Decarreau, W.D. Huff and an anonymous reviewer improved the text.

REFERENCES

Alt, J.C. (1999) Very low-grade hydrothermal metamorphism of basic igneous rocks. Pp. 169–201 in: *Low-grade Metamorphism* (M. Frey and D. Robinson, editors). Blackwell Science, Oxford, UK.

Bailey, S.W. (1980) Summary of recommendations of AIPEA nomenclature committee on clay minerals. *American Mineralogist*, **65**, 1–7.

Beaufort, D. and Meunier, A. (1994) Saponite, corrensite and chlorite-saponite mixed-layers in the Sancerre-Couy deep drill-hole (France). *Clay Minerals*, **29**, 47–61.

Besson, G., Drits, V.A., Daynyak, L.G. and Smoliar, B.B. (1987) Analysis of cation distribution in dioctahedral micaceous minerals on the basis of IR spectroscopy data. *Clay Minerals*, **22**, 465–478.

Blum, A.E. and Eberl, D.D. (2004) Measurement of clay surface areas by polyvinylpyrrolidone (PVP) sorption and its use for quantifying illite and smectite abundance. *Clays and Clay Minerals*, **52**, 589–602.

Bodine, M.W. Jr. and Madsen, B.M. (1987) Mixed layer chlorite/smectites from a Pennsylvanian evaporate cycle, Grand County, Utah. Pp. 85–93 in: *Proceedings of the International Clay Conference*, Denver (L.G. Schultz, H. van Olphen and F.A. Mumpton, editors). The Clay Minerals Society, Bloomington, Indiana.

Bosio, N.J., Hurst, V.J. and Smith, R.L. (1975) Nickeliferous nontronite, a 15 Å garnierite, at Niquelandia, Goias, Brazil. *Clays and Clay Minerals*, **23**, 400–403.

Brigatti, M.F. (1983) Relationships between composition and structure in Fe-rich smectites. *Clay Minerals*, **18**, 177–186.

Brindley, G.W. and Hang, P.T. (1973) The nature of garnierites – I structures, chemical compositions and color characteristics. *Clays and Clay Minerals*, **21**, 27–40.

Brindley, G.W. and Maksimovic, Z. (1974) The nature and nomenclature of hydrous nickel-containing silicates. *Clay Minerals*, **10**, 271–277.

Brindley, G.W. and Souza, J.V. (1975) Nickel-containing montmorillonites and chlorites from Brazil, with remarks on schuchardite. *Mineralogical Magazine*, **40**, 141–152.

Brindley, G.W., Bish, D.L. and Wan, H.-M. (1977) The nature of kerolite, its relation to talc and stevensite. *Mineralogical Magazine*, **41**, 443–452.

Brindley, G.W., Bish, D.L. and Wan, H.-M. (1979) Compositions, structures and properties of nickel-containing minerals in the kerolite-pimelite series. *American Mineralogist*, **64**, 615–625.

Chamley, H. (1989) *Clay Sedimentology*. Springer Verlag, Berlin, 623 pp.

Christidis, G.E. (2001) Formation and growth of smectites in bentonites: a case study from Kimolos Island, Aegean, Greece. *Clays and Clay Minerals*, **49**, 204–215.

Christidis, G.E. and Dunham, A.C. (1993) Compositional variations in smectites: Part I. Alteration of intermediate volcanic rocks. A case study from Milos Island, Greece. *Clay Minerals*,, **28**, 255–273.

Christidis, G. and Dunham, A.C. (1997) Compositional variations in smectites: Part II. Alteration of acidic precursors. A case study from Milos Island, Greece. *Clay Minerals*, **32**, 253–270.

Courtin, B. (1979) Etude geologique de la region de Domokos (Grece): le front des zones internes et les massifs ophiolitiques d'Othris occidentale. These 3^{e} cycle, Université de Lille, France.

Decarreau, A. (1985) Partition of divalent transition elements between octahedral sheets of trioctahedral smectites and water. *Geochimica et Cosmochimica Acta*, **49**, 1537–1544.

Decarreau, A., Colin, F., Herbillon, A., Manceau, A., Nahon, D., Paquet, H., Trauth-Badeaud, D. and Trescases, J.J. (1987) Domain segregation in Ni-Fe-Mg-smectites. *Clays and Clay Minerals*, **35**, 1–10.

Dijkstra, A., Drury, M. and Vissers, R. (2001) Structural petrology of plagioclase peridotites in the West Othrys Mountains (Greece): melt impregnation in mantle lithosphere. *Journal of Petrology*, **42**, 5–24.

Dubinska, E. (1986) Nickel-bearing ferric analogue of montmorillonite from weathering crust at Szklary near Zabkowice Slaskie (Lower Silesia). *Archiwum Mineralogiczne*, **41**, 35–47.

Dunham, A.C. and Wilkinson, F.C.F. (1978) Accuracy, precision and detection limits of energy-dispersive electron microprobe analysis of silicates. *X-ray Spectrometry*, **7**, 50–56.

Eberl, D.D., Jones, B.F. and Khoury, H.N. (1982) Mixed-layer kerolite/stevensite from the Amargosa Desert, Nevada. *Clays and Clay Minerals*, **30**, 321–326.

Eberl, D.D., Nuesch, R., Šuchá, V. and Tsipursky, S. (1998) Measurement of fundamental particle thicknesses by X-ray diffraction using PVP-10 intercalation. *Clays and Clay Minerals*, **46**, 89–97.

Gaudin, A., Grauby, O., Noack, N., Decarreau, A. and Petit, S. (2004a) Accurate crystal chemistry of ferric smectites from the lateritic nickel ore of Murrin Murrin (Western Australia). I. XRD and multi-scale chemical approaches. *Clay Minerals*, **39**, 301–315.

Gaudin, A., Petit, S., Rose, J., Martin, F., Decarreau, A., Noack, N. and Borschneck, D. (2004b) The accurate crystal chemistry of ferric smectites from the lateritic nickel ore of

Murrin Murrin (Western Australia). II. Spectroscopic (IR and EXAFS) approaches. *Clay Minerals*, **39**, 453–467.

Gerard, P. and Herbillon, A.J. (1983) Infrared studies of Ni-bearing clay minerals of the kerolite-pimelite series. *Clays and Clay Minerals*, **31**, 143–151.

Grim, R.E. and Güven, N. (1978) *Bentonites. Geology, Mineralogy, Properties and Uses*. Elsevier, Amsterdam, pp. 143–155.

Golightly, J.P. (1981) *Nickeliferous Laterite Deposits*. *Economic Geology*, 75th Anniversary Volume, pp. 710–735.

Güven, N. (1988) Smectite. Pp 497–559 in: *Hydrous Phyllosilicates* (S.W. Bailey, editor). Reviews in Mineralogy, **19**. Mineralogical Society of America, Washington, D.C.

Herbillon, A.J., Frankart, R. and Vielvoye, L. (1981) An occurrence of interstratified kaolinite-smectite minerals in a red-black soil toposequence. *Clay Minerals*, **16**, 195–201.

Hynes, A. (1972) The geology of part of the western Othrys Mountain, Greece. Unpublished PhD thesis, University of Cambridge, UK.

Inoue, A., Meunier, A. and Beaufort, A. (2004) Illite-smectite mixed-layer minerals in felsic volcaniclastic rocks from drill cores, Kakkonda, Japan. *Clays and Clay Minerals*, **52**, 66–84.

Jones, B.F. and Weir, A.H. (1983) Clay minerals of Lake Albert, an alkaline, saline lake. *Clays and Clay Minerals*, **31**, 161–172.

Konstantopoulou, G. and Rassios, A. (1993) Application in the Othrys area. Pp. 96–102 in: *Advanced Tectonic and Geochemical Methods for Chrome Exploration in Ophiolites*. Contract MA2M-CT90-0035, Final Technical Report.

Köster, H.M. (1982) The crystal structure of 2:1 layer silicates. Pp. 41–71 in: *Proceedings of the International Clay Conference*, Pavia, Italy (H. van Olphen and F. Veniale, editors).

Lippmann, F. (1982) The thermodynamic status of clay minerals. Pp. 475–485 in: *Proceedings of the International Clay Conference*, Pavia, Italy (H. van Olphen and F. Veniale, editors).

Manceau, E. and Calas, G. (1986) Nickel-bearing clay minerals: II. Intracrystalline distribution of nickel: an X-ray absorption study. *Clay Minerals*, **21**, 341–360.

Manceau, A., Calas, G. and Decarreau, A. (1985) Nickel-bearing clay minerals: I. Optical spectroscopic study of nickel crystal chemistry. *Clay Minerals*, **20**, 367–387.

May, H.M., Kinniburgh, D.G., Helmke, P.A. and Jackson, M.L. (1986) Aqueous dissolution, solubilities and thermodynamic stabilities of common aluminosilicate clay minerals; kaolinite and smectite. *Geochimica et Cosmochimica Acta*, **50**, 1667–1677.

Menzies, M. (1973) Mineralogy and partial melt textures within an ultramafic-mafic body, Greece. *Contributions to Mineralogy and Petrology*, **43**, 273–285.

Mitsis, I. (2001) Mineralization of nickel minerals, magnetite and apatite in the Ano Agoriani region, Othrys, Greece. PhD thesis, University of Athens, Greece (in Greek).

Mitsis, I. and Economou-Eliopoulos, M. (2001) Occurrence of apatite associated with magnetite in an ophiolite complex (Othrys), Greece. *American Mineralogist*, **86**, 1143–1150.

Nahon, D., Colin, F. and Tardy, Y. (1982) Formation and distribution of Mg, Fe, Mn-smectites in the first stages of the lateritic weathering of forsterite and tephroite. *Clay Minerals*, **17**, 339–348.

Nisbet, E. (1974) The geology of the Neraida area, Othrys Mountains, Greece. Unpublished PhD thesis, University of Cambridge, UK.

Paquet, H., Duplay, J. and Nahon, D. (1982) Variations in the composition of phyllosilicates monoparticles in a weathering profile of ultrabasic rocks. Pp. 595–603 in: *Proceedings of the International Clay Conference*, Pavia, Italy (H. van Olphen and F. Veniale, editors).

Reynolds, R.C. Jr and Reynolds, R.C. III (1996) *Newmod-for-Windows. The calculation of one-dimensional X-ray diffraction patterns of mixed-layered clay minerals*. Published by the authors, Hanover, New Hampshire, USA.

Russell, J.D. (1987) Infrared methods. Pp 133–173 in: *A Handbook of Determinative Methods in Clay Mineralogy* (M.J. Wilson, editor). Blackie, Glasgow and London.

Sakharov, B., Dubinska, E., Bylina, P., Kozubowski, J.A., Kapron, G. and Frontczak-Banewicz, M. (2004) Serpentine-smectite interstratified minerals from Lower Silesia (SW Poland). *Clays and Clay Minerals*, **52**, 55–65.

Shimoda, S. (1971) Mineralogical studies of a species of stevensite from the Obori mine, Yamagata Prefecture, Japan. *Clay Minerals*, **9**, 185–192.

Slonimskaya, M.V., Besson, G., Dainyak, L.G., Tchoubar, C. and Drits, V. (1986) Interpretation of the IR spectra of celadonites and glauconites in the region of OH-stretching frequencies. *Clay Minerals*, **21**, 377–388.

Środoń, J. and Eberl, D.D. (1984) Illite. Pp. 495–544 in: *Micas* (S.W. Bailey, editor). Reviews in Mineralogy, **13**. Mineralogical Society of America, Washington, D.C.

Wiéwióra, A., Dubinska, E. and Iwasinska, I. (1982) Mixed-layering in Ni-containing talc-like minerals from Szklary, Lower Silesia, Poland. Pp. 111–125 in: *Proceedings of the International Clay Conference*, Pavia, Italy (H. van Olphen and F. Veniale, editors).

Wilkins, R.W.T. and Ito, J. (1967) Infrared spectra of some synthetic talcs. *American Mineralogist*, **52**, 1649–1661.

Wilson, M.J. (1987) Soil smectites and related interstratified minerals: Recent developments. Pp. 167–173 in: *Proceedings of the International Clay Conference* Denver (L.G. Schultz, H. van Olphen and F.A. Mumpton, editors). The Clay Minerals Society, Bloomington, Indiana.

Zhou, Z. and Fyfe, W.S. (1989) Palagonization of basaltic glass of DSPD Site 335, Leg 37: Textures, chemical composition and mechanism of formation. *American Mineralogist*, **74**, 1045–1053.

(*Received 3 November 2005; revised 20 July 2006; Ms. 1105; A.E. Warren D. Huff*)